STANFORD RESEARCH INSTITUTE
Menlo Park, California 94025 · U.S.A.

NASA CR-66798

STUDY OF STRAIN-HARDENING NEAR CRACK TIPS

By Bill R. Baker
and Yapa D. S. Rajapakse

Prepared under Contract No. NAS1-8032
STANFORD RESEARCH INSTITUTE
Menlo Park, California

for

NATIONAL AERONAUTICS AND SPACE ADMINISTRATION

STUDY OF STRAIN-HARDENING NEAR CRACK TIPS

ABSTRACT

A nonlinear integral equation approach is developed for the elastic-plastic analysis of stresses and strains near crack tips. This approach is potentially useful for numerical methods of calculation. If the elastic solution is known, the finite difference network does not have to encompass the complete body, but only needs to include the plastic zone to obtain the plastic part of the solution.

Attempts to use this technique to generate simplified models of the material behavior at the crack tip and thereby develop simplified failure criteria were not successful. This work revealed the importance of the description of the microstructure in the region where the crack propagates. It is concluded that this description is as essential as the strain-hardening continuum representation of the material for the establishment of a useful failure criterion.

Table of Contents

Introduction

Efficient structural engineering design requires a good understanding of failure and fracture mechanisms. Fracture in brittle elastic materials has been fairly well described by stress analysis based upon the linear theory of elasticity combined with a failure criterion of Griffith [14].

Griffith's criterion has also been widely used in a form based upon the stress intensity factor. The success of such methods, involving infinite stresses in the mathematical analysis, has been given a more palatable physical interpretation by Barenblatt [16]. Barenblatt has essentially provided a simple way to introduce a measure of the intermolecular forces or microstructure into the continuum model of linear elasticity.

The stress intensity factor criterion does not agree well with experimental results for more ductile materials where noticeable plastic strain occurs. An important step toward a description of plastic yielding at a crack was introduced by Dugdale [10]. The analysis, based upon the initial yield stress of the material, successfully predicts the size of the yield zone. However, the Dugdale model does not provide a failure criterion.

When the present investigation was started it was hoped that modification of the Dugdale model to include a strain hardening description of the material could be used to obtain a failure criterion. The approximate methods of stress analysis for the nonlinear continuum given in this report are still very crude and must be refined.

However, initial attempts at analysis have led to the conclusion that not only the strain hardening properties of the continuum but also a description of the microstructure at a crack tip will be necessary to establish a failure criterion for a ductile material. Since the problem is nonlinear there is little chance that a stress concentration factor method can be used.

I. General Relationships

Deformation Theory of Plasticity

In this chapter we will formulate the general stress-strain relations for a linearly strain hardening material under conditions of proportional loading. That is, the discussion is one of the deformation theory of plasticity. Deformation theory provides definite stress-strain relations which simplify the mathematical analysis. It has been used by Rice [1, 2] for the solution of several problems of longitudinal shear near notches and cracks. It has also been used by Hutchinson [3, 4] and Rice and Rosengren [5] in the study of a type of stress singularity near a crack. Budiansky [6] has suggested that the deformation theory also provides a good description of stress and strain distributions in many cases where the requirements of proportional loading are not met.

In the case of proportional loading the strain rates can be integrated to give a one to one correspondence between the plastic strains ϵ_{ij}^{P} and the stress deviator components s_{ij}. The form given by Mendelson [7] is

$$\epsilon_{ij}^{p} = \frac{3}{2}\frac{\epsilon_p}{\sigma_e} s_{ij} \tag{1.1}$$

where the effective stress is

$$\sigma_e = \sqrt{3J_2} = \sqrt{3s_{ij}s_{ij}} = \frac{1}{\sqrt{2}}[(\sigma_x-\sigma_y)^2 + (\sigma_y-\sigma_z)^2 + (\sigma_z-\sigma_x)^2 + 6(\tau_{xy}^2+\tau_{yz}^2+\tau_{xz}^2)]^{1/2} \tag{1.2}$$

and ϵ_p is the total plastic strain.

If we refer to the relationship between effective stress σ_e and total strain ϵ sketched in Fig. 1.1, we can express the secant modulus E_s as the ratio of effective stress to total strain, or

$$E_s = \frac{\sigma_e}{\epsilon} = (1 - \frac{\epsilon^p}{\epsilon}) E$$

where E is Young's modulus of elasticity. Now eq. (1.1) can be written as

$$\epsilon^p_{ij} = \frac{3}{2}(\frac{1}{E_s} - \frac{1}{E}) s_{ij} = \frac{3}{2} \lambda_o s_{ij} = \frac{\lambda}{2G} s_{ij} \qquad (1.3)$$

where

$$\lambda_o = \frac{1}{E_s} - \frac{1}{E}$$

$$\lambda = 3G \lambda_o = 3G(\frac{1}{E_s} - \frac{1}{E}) \qquad (1.4)$$

Note that if $\sigma_e < \sigma_o$, the initial yield stress in simple tension, then $E_s = E$ and $\lambda_o = \lambda = 0$. The initial yield stress in pure shear τ_o is given by

$$\tau_o = \sigma_o/\sqrt{3} \qquad (1.5)$$

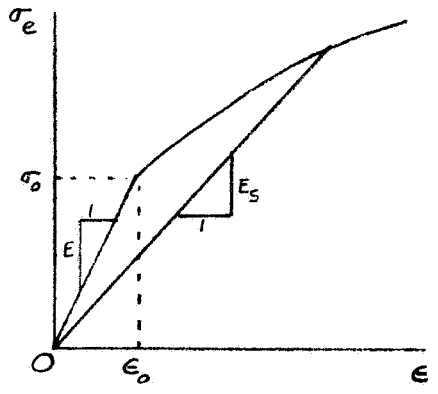

Fig. 1.1

Effective stress vs total strain

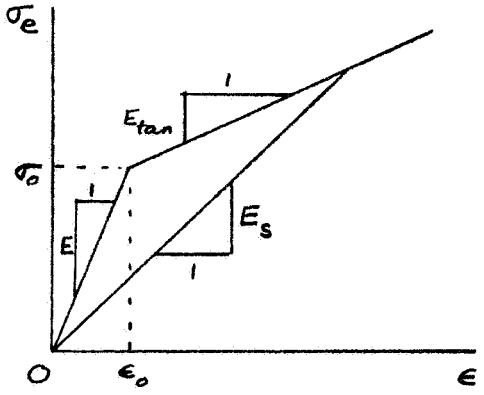

Fig. 1.2

Characteristic of linear strain hardening

For a material which strain **hardens** linearly, i.e., for a material having a bilinear effective stress-total strain curve (Fig. 1.2), the secant modulus E_s can be expressed in terms of the tangent modulus E_{tan} to give

$$\lambda_0 = \frac{1}{E_s} - \frac{1}{E} = (1-\frac{\sigma_0}{\sigma_e})(\frac{1}{E_{tan}} - \frac{1}{E})$$
$$\lambda = 3G\lambda_0 = 3G(1-\frac{\sigma_0}{\sigma_e})(\frac{1}{E_{tan}} - \frac{1}{E}) \tag{1.6}$$

where $\sigma_e > \sigma_0$. As before, $\lambda_0 = \lambda = 0$ when $\sigma_e \leq \sigma_0$.

Plane Stress

Here we consider the problem of plane stress. In a state of plane stress parallel to the xy plane, the stress components τ_{xz}, τ_{yz} and σ_z are all zero. Thus, the effective stress is

$$\sigma_e = (\sigma_x^2 + \sigma_y^2 - \sigma_x\sigma_y + 3\tau_{xy}^2)^{1/2} \tag{1.7}$$

The basic stress-strain relations are,

$$\epsilon_x = \frac{\partial u}{\partial x} = \frac{1}{E}(\sigma_x - \nu\sigma_y) + \lambda_0(\sigma_x - \frac{1}{2}\sigma_y)$$
$$\epsilon_y = \frac{\partial v}{\partial y} = \frac{1}{E}(\sigma_y - \nu\sigma_x) + \lambda_0(\sigma_y - \frac{1}{2}\sigma_x) \tag{1.8}$$
$$\epsilon_{xy} = \frac{1}{2}\left(\frac{\partial u}{\partial y} + \frac{\partial v}{\partial x}\right) = \frac{1}{2G}\tau_{xy} + \frac{3}{2}\lambda_0\tau_{xy}$$

where λ_0 is given by (1.4) in terms of the Young's modulus E and the current value of the secant modulus E_s.

The nonzero stress components σ_x, σ_y, τ_{xy} satisfy the two equations of equilibrium

$$\frac{\partial \sigma_x}{\partial x} + \frac{\partial \tau_{xy}}{\partial y} = 0$$

$$\frac{\partial \tau_{xy}}{\partial x} + \frac{\partial \sigma_y}{\partial y} = 0 \tag{1.9}$$

These equations are identically satisfied if we express the stress components in terms of the Airy stress function φ:

$$\sigma_x = \varphi_{yy}, \quad \sigma_y = \varphi_{xx}, \quad \tau_{xy} = -\varphi_{xy} \tag{1.10}$$

The strain components ϵ_x, ϵ_y, ϵ_{xy} satisfy the compatibility equation

$$\frac{\partial^2 \epsilon_x}{\partial y^2} + \frac{\partial^2 \epsilon_y}{\partial x^2} = 2 \frac{\partial^2 \epsilon_{xy}}{\partial x \partial y} \tag{1.11}$$

The compatibility equation expressed in terms of φ reads

$$\frac{1}{E} \nabla^2 \nabla^2 \varphi = -[\lambda_0 (\sigma_x - \tfrac{1}{2}\sigma_y)]_{,yy} - [\lambda_0 (\sigma_y - \tfrac{1}{2}\sigma_x)]_{,xx} + 3[\lambda_0 \tau_{xy}]_{,xy} \tag{1.12}$$

Transverse Shear

In the case of transverse shear the only nonvanishing displacement component is w, normal to the xy plane. Therefore, the only nonzero stress components are τ_{xz} and τ_{yz}, which will be abbreviated to τ_x and τ_y. The effective stress expressed in terms of these 2 stress components is

$$\sigma_e = \sqrt{3}\, (\tau_x^2 + \tau_y^2)^{1/2} \tag{1.13}$$

The nonvanishing strain components are

$$\epsilon_{xz} = \frac{1}{2}\frac{\partial w}{\partial x} = \frac{\tau_x}{2G} + \epsilon^p_{xz} = \frac{\tau_x}{2G}(1+\lambda)$$

$$\epsilon_{yz} = \frac{1}{2}\frac{\partial w}{\partial y} = \frac{\tau_y}{2G} + \epsilon^p_{yz} = \frac{\tau_y}{2G}(1+\lambda) \tag{1.14}$$

The compatibility equation obtained by eliminating w from the last two equations is

$$\frac{\partial}{\partial x}[\tau_y(1+\lambda)] = \frac{\partial}{\partial y}[\tau_x(1+\lambda)] \tag{1.15}$$

The only equilibrium equation which is not satisfied identically is the one for forces acting normal to the x-y plane

$$\frac{\partial \tau_x}{\partial x} + \frac{\partial \tau_y}{\partial y} = 0 \tag{1.16}$$

This equilibrium equation is satisfied by the choice of a stress potential φ where

$$\tau_x = \frac{\partial \varphi}{\partial y} \quad , \quad \tau_y = -\frac{\partial \varphi}{\partial x} \tag{1.17}$$

Substitution of equations (1.17) into (1.16) gives the compatibility equation for the stress function φ

$$(1+\lambda)\nabla^2 \varphi + \frac{\partial \varphi}{\partial x}\frac{\partial \lambda}{\partial x} + \frac{\partial \varphi}{\partial y}\frac{\partial \lambda}{\partial y} = 0 \tag{1.18}$$

In the case of linear strain hardening

$$\lambda = \begin{cases} 0 & \tau \leq \tau_o \\ \beta(1 - \frac{\tau_o}{\tau}) & \tau > \tau_o \end{cases} \tag{1.19}$$

where

$$\beta = 3G(\frac{1}{E_{tan}} - \frac{1}{E}) \tag{1.20}$$

and

$$\tau = (\tau_x^2 + \tau_y^2)^{1/2} = (\varphi_x^2 + \varphi_y^2)^{1/2} \tag{1.21}$$

Transverse Shear: Elastic Solution for Half Space

We consider the half space $y \geq 0$ with the following transverse shear boundary loading at the face $y = 0$:

$$\tau_y = \tau_{yz} = \begin{cases} \sum_{n=0}^{N} c_n x^n & |x| < a \\ 0 & |x| > a \end{cases} \tag{1.22}$$

Assuming that there is no yielding (i.e., for the fully elastic problem), we can write the stress components at a point $z = x + iy$ (not to be confused with the z coordinate) in the form

$$F(z) = \tau_y + i\,\tau_x \tag{1.23}$$

where the complex stress function $F(z)$ is given in terms of the boundary loading τ_y by

$$F(z) = \frac{1}{\pi i} \int_{-\infty}^{+\infty} \frac{\tau_y(t)}{t-z}\, dt \tag{1.24}$$

For the polynomial loading given above, the following complex stress function is obtained

$$F(z) = \frac{1}{\pi i} \left(\ln \frac{z-a}{z+a}\right) \sum_{n=0}^{N} c_n z^n + \frac{2}{\pi i} \sum_{n=0}^{N} c_n S_n \tag{1.25}$$

where

$$S_n = \sum_{i=1}^{\left[\frac{n+1}{2}\right]} \frac{z^{n-2i+1} a^{2i-1}}{2i-1} \tag{1.26}$$

and $\left[\frac{n+1}{2}\right]$ denotes the integral part of $(n+1)/2$.

We shall later examine in detail the above problem with the parabolic shear loading

$$\tau_y = \begin{cases} \tau_m(1 - x^2) & |x| < 1, \quad y = 0 \\ 0 & |x| > 1, \quad y = 0 \end{cases} \tag{1.27}$$

The fully elastic solution for this loading is

$$F_e(z) = \tau_y + i\,\tau_x = \frac{\tau_m}{\pi i}\{(1-z^2)\ln \frac{z-1}{z+1} - 2z\} \tag{1.28}$$

The indefinite integral of $F_e(z)$ gives

$$F_{eo}(z) = \varphi_e + iGw = \frac{\tau_m}{\pi i}[(2+z)(1-z^2)\ln(z-1) + (2-z)(z+1)^2\ln(z+1) + 2z^2] + \text{const} \tag{1.29}$$

whose real part gives the elastic stress function $\varphi_e(x,y)$ and the imaginary part gives the displacement component $w(x,y)$ times the elastic modulus G.

II An Integral Equation Formulation

The Transverse Shear Problem

We will now examine the partial differential equation (1.8) for transverse shear and develop a numerical method for its solution based upon an integral equation formulation. The compatibility equation is

$$\nabla^2\varphi = \frac{\partial}{\partial x}(\lambda\tau_y) - \frac{\partial}{\partial y}(\lambda\tau_x) \equiv \rho(x,y) \tag{2.1}$$

Various iterative techniques have been developed for the solution of non-linear equations of this form. Most of the methods consist of a process in which the right hand side of the equation is calculated from a previous approximate solution. From this known "inhomogeneous term" a new approximation for φ is found, and it is used to determine the right hand side for the next step of the iteration.

The process is continued until successive solutions differ only slightly or appear to have converged to the limiting solution. Of course, the boundary conditions are satisfied at each step of the iteration. For the first step the elastic solution is chosen where all plasticity effects are ignored .

The material considered in Chapter I behaves like a linear elastic solid if the effective stress remains below the initial yield stress σ_o. Therefore, λ is identically zero and (2.1) reduces to Laplace's equation in the elastic region. That is, φ is a harmonic function in the elastic zone.

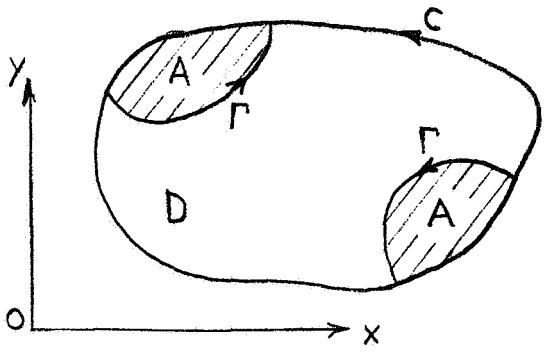

Fig. 2.1 The Body D with Plastic Region A.

By using the Green's function $G(P;Q)$, see Sneddon [8], the partial differential equation (2.1) and its boundary conditions can be transformed into an equivalent integral equation. The Green's function has the form

$$2\pi\, G(P;Q) = -\ln r_{PQ} + V \tag{2.2}$$

where r_{PQ} is the distance between the source point Q at (ξ,η) and the observation point P at (x,y). The harmonic function V is regular in all of the region D and is chosen so that the Green's function vanishes if P is on the boundary C of the region:

$$G(P;Q) \equiv 0 \quad \text{if} \quad P \in C \tag{2.3}$$

It can also be shown that the Green's function is symmetric or

$$G(P;Q) = G(Q;P) \tag{2.4}$$

The right hand side of equation (2.1) can be considered to be a distribution of sources. Then a solution of the inhomogeneous equation is given by the Poisson integral with the fundamental singular solution $-(\ln r_{PQ})/2\pi$ as kernel.

$$\varphi_1(P) = \int_D - \frac{\ln r_{PQ}}{2\pi} \rho(\xi,\eta)d\xi d\eta \tag{2.5}$$

However, if we use the complete Green's function of equation (2.2) as kernel then the integral not only is an inhomogeneous solution of equation (2.1), but because of property (2.3) it follows that the integral also vanishes identically if P is on the boundary.

We can also add an elastic solution φ_e (corresponding to $\rho \equiv 0$ in (2.1)) in order to write the general solution as

$$\varphi(P) = \int_D G(P;Q)\left[\frac{\partial}{\partial\eta}(\lambda\tau_x) - \frac{\partial}{\partial\xi}(\lambda\tau_y)\right]d\xi d\eta + \varphi_e(P) \tag{2.6}$$

Since λ is identically zero in the elastic regions, the integration in the last equation need only be extended over the plastic region A. Also the integral vanishes if P lies on the boundary, so the elastic solution φ_e must be chosen to satisfy the given boundary conditions.

If the domain D is infinite then the harmonic function V can be chosen so that the Green's function vanishes at infinity like r^{-1}. Then it can be shown that the total stress function φ is dominated by φ_e for points far from the plastic zone.

Before developing an iterative method of solution it is desirable to integrate by parts to eliminate the derivatives of stresses in equation (2.6). Since $G(P;Q)$ vanishes if Q lies on the boundary C and $\lambda(Q)$ vanishes if Q lies on the elastic-plastic interface Γ, the integrated terms are all zero, and we obtain

$$\varphi(P) = \int_A \lambda(Q)\left[\tau_y(Q)\,\frac{\partial G}{\partial\xi}\,(P;Q) - \tau_x(Q)\,\frac{\partial G}{\partial\eta}\,(P;Q)\right]dA_Q + \varphi_e(P) \tag{2.7}$$

It is convenient to use complex function notation here even though the stress function is not harmonic in the plastic region. We will consider a specific case of a half-plane $y \geq 0$ where boundary stresses τ_y are applied on a portion of the x-axis. The half-plane is sketched in Fig. 2.2 with the observation point P at (x,y) the source point Q at (ξ,η) and the image point $\bar{Q}$ at $(\xi,-\eta)$.

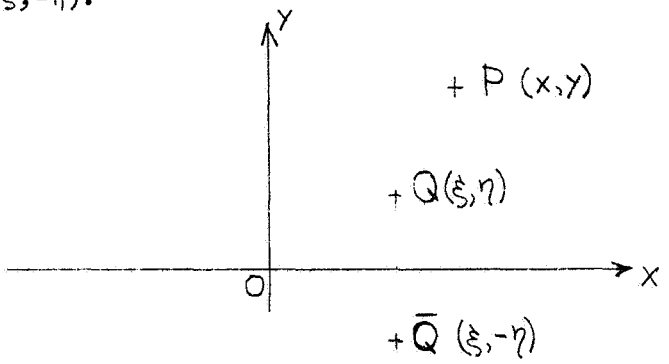

Fig. 2.2 Observation, source and image points for the half-plane

The Green's function can be constructed by the classical method of images. The source of unit strength at Q and a source of strength -1 at the image point $\bar{Q}$ results in zero value on $y = 0$. Therefore, the Green's function is

$$G(P;Q) = \frac{1}{2\pi} [-\ln r_{PQ} + \ln r_{P\bar{Q}}] \tag{2.8}$$

We use the usual complex variable $z = x + iy$ and introduce the notation

$$z_P = x + iy, \quad z_Q = \xi + i\eta, \quad z_{\bar{Q}} = \xi - i\eta$$

$$z_{PQ} = z_P - z_Q = x - \xi + i(y-\eta), \quad z_{P\bar{Q}} = z_P - z_{\bar{Q}} = x - \xi + i(y+\eta) \tag{2.9}$$

$$S(z_{PQ}) = -\frac{\ln(z_{PQ})}{2\pi}, \quad R(z_{P\bar{Q}}) = -\frac{\ln(z_{P\bar{Q}})}{2\pi}$$

The function R is analytic and single valued with respect to z_P if P lies in the upper half-plane, but S has a branch point at $z_P = z_Q$. Nevertheless, the real parts of both these functions are single valued. It is convenient to write the Green's function as

$$G(P;Q) = \mathrm{Re}(S-R) \tag{2.10}$$

Derivatives of the Green's function which appear in the integral equation are

$$\begin{aligned}
\frac{\partial S}{\partial x} &= -\frac{\partial S}{\partial \xi} = \frac{dS(z_{PQ})}{dz_{PQ}} \equiv S' = -\frac{1}{2\pi z_{PQ}} \\
\frac{\partial R}{\partial x} &= -\frac{\partial R}{\partial \xi} = \frac{dR(z_{P\bar{Q}})}{dz_{P\bar{Q}}} \equiv R' = -\frac{1}{2\pi z_{P\bar{Q}}} \\
\frac{\partial S}{\partial y} &= -\frac{\partial S}{\partial \eta} = iS' \\
\frac{\partial R}{\partial y} &= \frac{\partial R}{\partial \eta} = iR'
\end{aligned} \tag{2.11}$$

Substitution of these results into (2.7) gives

$$\varphi(P) = \mathrm{Re} \int_A \lambda[(i\tau_x - \tau_y)S' + (i\tau_x + \tau_y)R']dA_Q + \varphi_e(P) \tag{2.12}$$

The elastic solution φ_e is obtained by ignoring plasticity effects or by formally setting λ equal zero in equation (2.1). Therefore φ_e is a solution of Laplace's equation, and it can be represented as the real part of an analytic single-valued function of the complex variable z_P. However,

such a representation is generally not valid for the total stress potential φ because $\lambda \neq 0$ in the plastic zone. Nevertheless, it is convenient to introduce a pseudocomplementary real function Ψ and write the complex integral (2.12) as

$$\varphi(P) - \varphi_e(P) + i\Psi(P) = \int_A \lambda[(i\tau_x - \tau_y)S'(P;Q) + (i\tau_x - \tau_y)R'(P;Q)]dA_Q \qquad (2.13)$$

If the observation point does not lie in the plastic zone A ($P \notin A$), then the functions S' and R' are analytic bounded functions of z_P and so are their derivatives. Then equation (2.13) can be differentiated with respect to x and y to obtain the following results.

$$\varphi_{,x}(P) - \varphi_{e,x}(P) + i\Psi_{,x}(P) = \int_A \lambda[(i\tau_x - \tau_y)S'' + (i\tau_x + \tau_y)R'']dA_Q$$

$$\varphi_{,y}(P) - \varphi_{e,y}(P) + i\Psi_{,y}(P) = \int_A \lambda[(i\tau_x - \tau_y)iS'' + (i\tau_x + \tau_y)iR'']dA_Q \ , \ P \notin A \qquad (2.14)$$

In fact, the last portions of these integrals even converge if $P \in A$ because $\overline{Q}$ is always in the lower half-plane, and $z_{P\overline{Q}}$ can never vanish. However, the second derivative of the singular term S is so strong that the first part of the integral (2.14) would not exist for $P \in A$.

Instead, as shown in the Appendix, we must first extract a small neighborhood of the point P from the area of integration in equation (2.13) before differentiating. The contribution of that small neighborhood is estimated and then differentiated. Direct differentiation of the remaining integral over the punctured domain A' can be carried out as in equation (2.14). The sums of the two contributions are

$$\varphi_{,x}(P) - \varphi_{e,x}(P) + i\Psi_{,x}(P) = -\frac{\lambda(P)\bar{D}(P)}{2} + \int_{A'} \lambda\bar{D}S''\, dA_Q - \int_A \lambda DR''dA_Q$$

$$\varphi_{,y}(P) - \varphi_{e,y}(P) + i\Psi_{,y}(P) = i\{-\frac{\lambda(P)\bar{D}(P)}{2} + \int_{A'} \lambda\bar{D}S''dA_Q - \int_A \lambda DR''dA_Q\} \tag{2.15}$$

where

$$D \equiv -\tau_y - i\tau_x = \varphi_{,x} - i\varphi_{,y} \qquad D_e \equiv -\tau_{ye} - i\tau_{xe} = \varphi_{e,x} - i\varphi_{e,y} \tag{2.16}$$

and the bar over a quantity denotes its complex conjugate. The integral over A' in equations (2.15) denotes the limit of the integral as the punctured plastic domain is shrunk down about the singular point P.

Elimination of the function Ψ from equations (2.15) gives

$$D(P) - D_e(P) = -\frac{\lambda(P)\bar{D}(P)}{2} + \int_{A'} \lambda\bar{D}S''dA_Q - \int_A \lambda DR''dA_Q \tag{2.17}$$

The last two integrals and D_e are analytic functions of z_P, but the first term of the right hand side shows that D is not analytic if P is in the plastic zone A. However, for points outside the plastic zone the function λ vanishes identically, the region A' is the entire plastic zone A, and equation (2.17) coincides with the results (2.14) for the elastic region.

A Numerical Solution

An approximate numerical scheme for the solution of the non-linear integral equation (2.17) will be described for a half-plane $y \geq 0$ loaded by a parabolic distribution of stress τ_y on $y = 0$. The starting values of the iterative scheme are given by the elastic solution of equation (1.28).

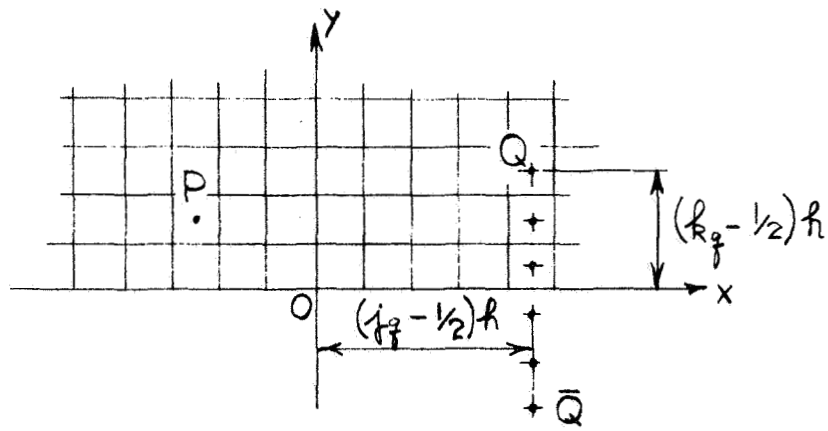

Fig. 2.1 The Grid for the Numerical Scheme

As sketched in Fig. 2.1 a grid is defined over a region of the half-plane large enough to include the expected plastic region. The stresses in each square are assumed to be constant and equal to the values at the midpoint of the mesh. The size of the squares is

$$dx = dy = h \tag{2.18}$$

The coordinates of an observation point P are now given in terms of integers j_P and k_P as follows:

$$x_P = (j_P - 1/2)h \qquad y_P = (k_P - 1/2)h \tag{2.19}$$

The integrals of (2.17) are approximated by finite sums. The weights attached to the complex stresses $D = -\tau_y - i\tau_x$ for each element of area in the integral are

$$SA(P,Q) \equiv S''(z_{PQ})dA_Q = \frac{h^2}{2\pi(z_{PQ})^2} = \frac{1}{2\pi}\frac{1}{[j_d + ik_d]^2}$$

$$RA(P,Q) \equiv R''(z_{P\bar{Q}})dA_Q = \frac{h^2}{2\pi(z_{P\bar{Q}})^2} = \frac{1}{2\pi}\frac{1}{[j_d + i(k_s-1)]^2} \tag{2.20}$$

where the differences and sum of the integer coordinates are

$$j_d = j_P - j_Q \qquad k_d = k_P - k_Q \qquad k_s = k_P + k_Q \tag{2.21}$$

Now the integral equation (2.17) can be written in finite form

$$D(P)[1 + \lambda(P)RA(P,P)] + \frac{1}{2}\lambda(P)\bar{D}(P) = D_e(P) + \Sigma'\lambda(Q)[\bar{D}(Q)SA(P,Q) - D(Q)RA(P,Q)] \tag{2.22}$$

where the summation symbol with a prime indicates that all values of Q are included except $Q = P$.

Some example calculations were carried out for a linearly strain hardening material of the type discussed in Chapter I. The stresses were computed in dimensionless form with τ_o, the initial yield stress in shear, as reference. The level of strain hardening is described by λ where

$$\lambda = \begin{cases} 0 & \tau \leq 1 \\ \beta(1-\frac{1}{\tau}) & , \quad \tau > 1 \end{cases} \tag{2.23}$$

and

$$\tau = \sqrt{\tau_x^2 + \tau_y^2} = |D| \qquad (2.24)$$

Calculations were coded in FORTRAN IV so that the complex arithmetic could be implemented directly in the program.

A simple point-wise iterative scheme was used for the solution of the system (2.22). First the constant influence functions $RA(P,Q)$ and $SA(P,Q)$ of equation (2.20) were calculated for a sufficient range of the integers j_d, k_d, and k_s. Then the basic elastic solution D_e, given in Chapter I for a parabolic distribution of load, was calculated and stored.

At each step of the iterative scheme the values of λ were calculated from the stresses of the preceding step. Hence, for the first iteration λ was calculated from the elastic solution. For each point P the right hand side of (2.22) was evaluated and the new value of $D(P)$ was calculated. This new value of $D(P)$ and the corresponding new value of $\lambda(P)$ were then stored.

This simple point by point relaxation method converges if β is very small, say $\beta \leq 1$. This corresponds to a very rapid rate of strain hardening; for example if $\beta = 1$ and $E \doteq 3G$ then $E \doteq 2E_t$. It probably would be possible to develop better methods involving simultaneous solution of equations (2.22) for several points P, say for all the points in one column of the grid. Such column relaxation methods would probably be more useful for cases of large β or small strain hardening.

An advantage of the integral equation method is that only values of stresses within the plastic region need be considered. A disadvantage is that there is coupling with all elements in the plastic zone, so each step of the iteration involves many calculations.

Integral Equation for Plane Stress

An equivalent integral equation formulation can also be given for the plane stress equation (1.12)

$$\nabla^2\nabla^2\varphi = -[\lambda_1(\sigma_x - \frac{\sigma_y}{2})]_{,yy} - [\lambda_1(\sigma_y - \frac{\sigma_x}{2})]_{,xx} + 3[\lambda_1\tau_{xy}]_{,xy} \equiv p(x,y)$$

where

$$\lambda_1 = E\,\lambda_o \tag{2.25}$$

The development parallels that of the problem of transverse shear except that the Green's function for the biharmonic problem must be used. The form is

$$G(P;Q) = G(x,y;\xi,\eta) = \frac{r_{PQ}^2 \ln r_{PQ}^2}{16\pi} + V \tag{2.26}$$

In this case V is a regular biharmonic function in the region D, and V is chosen so that the Green's function G and its normal derivative vanish on the boundary C.

The Green's function for the biharmonic problem is the influence function for the transverse bending of plates. It represents the product of the bending modulus times the deflection at point P due to a unit load acting at Q when the boundaries of the plate are clamped.

Now we consider that the right hand side of equation (2.25) represents a distributed transverse load. The total deflection due to that distributed load with the edges of the plate clamped is

$$w_1(P) = \int_A G(P;Q)\, p(Q)\, dA_Q \tag{2.27}$$

In addition we may superpose a solution of the homogeneous equation where $\rho(x,y) \equiv 0$. This biharmonic function φ_e can be adjusted to satisfy prescribed non-zero values of displacement and slope at the edge of the plate. The general solution is

$$\varphi(P) = \int_A G(P;Q)\{-[\lambda_1(\sigma_x - \frac{\sigma_y}{2})]_{,\eta\eta} - [\lambda_1(\sigma_y - \frac{\sigma_x}{2})]_{,\xi\xi} + 3[\lambda_1 \tau_{xy}]_{,\xi\eta}\} dA_Q + \varphi_e(P) \quad (2.28)$$

In terms of the plane stress problem the normal and tangential stresses due to the integral are zero, and the biharmonic function $\varphi_e(P)$ is the solution of the perfectly elastic problem computed for the given boundary stresses.

Approximate iterative techniques similar to those of the transverse shear problem could also be developed for the solution of the integral equation (2.28). In order to reduce the error created by differentiating the approximate quantities in the curly brackets, it is desirable to integrate by parts to shift the differentiation onto the Green's function which is known exactly.

Most of the integrated terms vanish because $G \equiv G_{,\xi} \equiv G_{,\eta} \equiv 0$ on the boundary C and $\lambda_1 \equiv 0$ on the elastic-plastic interface Γ. The remaining terms are

$$\varphi(P) = \int_\Gamma G\{-(\sigma_x - \frac{\sigma_y}{2})\lambda_{1,\eta} \sin\alpha - (\sigma_y - \frac{\sigma_x}{2})\lambda_{1,\xi} \cos\alpha + \frac{3}{2}\tau_{xy}(\lambda_{1,\eta}\cos\alpha + \lambda_{1,\xi}\sin\alpha)\} ds$$

$$+ \int_A \lambda_1\{-(\sigma_x - \frac{\sigma_y}{2})G_{,\eta\eta} - (\sigma_y - \frac{\sigma_x}{2})G_{,\xi\xi} + 3\tau_{xy}G_{,\xi\eta}\} dA + \varphi_e(P) \quad (2.29)$$

where α is the angle between the x-axis and the exterior normal of the plastic region.

From the basic properties of the Green's function it follows that the first integral is a regular biharmonic function if P is not on Γ, and the integral and its normal derivative vanish if P lies on the boundary C. Furthermore, the integral and its normal derivative are continuous across Γ, so it follows that the first integral gives zero stresses in the entire region D and it can be omitted.

The second derivatives of the Green's function $G_{,\xi\xi}$ and $G_{,\eta\eta}$ include the singular term $\ln r_{PQ}$ which also occurs directly in the Green's function of the transverse shear problem. Stress components are obtained from the second derivatives of equation (2.29) so the singular logarithmic term must be treated by the puncturing technique used in the transverse shear problem and discussed in the Appendix.

II Appendix

If $P \in A$ then we can not differentiate the singular term of (2.13) directly. Instead we first break up the region of integration of the first term as follows:

$$I_1 \equiv \int_A \lambda(i\tau_x - \tau_y)S'(P;Q)dA_Q = \int_{A-C_o} fS'dA + \int_{C_o} fS'dA \qquad (A2.1)$$

where

$$f \equiv \lambda(i\tau_x - \tau_y) \qquad (A2.2)$$

and C_o is a small region, say a circle with radius ϵ and center P_o, such that $P \in C_o$. A circle of this type is sketched in Fig. A2.1.

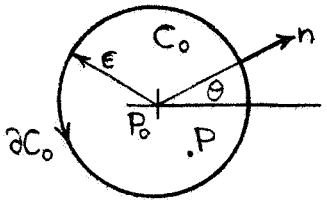

Fig. A2.1 A circular neighborhood containing P.

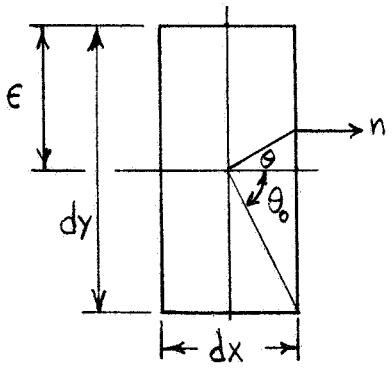

Fig. A2.2 A rectangular element

The next to last integral of A2.1 can be differentiated directly because P is not contained in the punctured domain. The result is that

$$I_{11} \equiv \int_{A-C_o} fS'dA \qquad (A2.3)$$

has the derivative

$$I'_{11} = \int_{A-C_o} fS''dA \tag{A2.4}$$

The remaining integral taken over the circle can be modified by integration by parts

$$I_{12} \equiv \int_{C_o} fS'd\xi d\eta = \int_{C_o} [-\frac{\partial}{\partial\xi}(fS) + \frac{\partial f}{\partial\xi} S]d\xi d\eta \tag{A2.5}$$

The last term of the last integral can be differentiated directly with respect to z_{PQ}, and its derivative is of the order $O[\epsilon]$. The next to last term of (A2.5) can be integrated to obtain

$$I_{13} = \int_{C_o} - \frac{\partial}{\partial\xi} [fS(z_{PQ})]d\xi d\eta = - \int_{\partial C_o} fS(z_{PQ})\cos\ (n,x)ds \tag{A2.6}$$

In the last integral it is emphasized that the angle between the exterior normal and the x-axis is being used even though it does coincide with the polar coordinate θ of the circle in Fig. A2.1. The distinction is of importance for the rectangular region of Fig. A2.2 which will be discussed later.

The last integral can now be differentiated with respect to z_{PQ}. Next we let P tend to P_o and expand the differentiable function f about its value f_o at P_o. The result is

$$I'_{13} = - \int_{\partial C_o} fS'(z_{PQ})\ \cos\ (n,x)ds = \frac{1}{2\pi} \int_0^{2\pi} \{f_o + O[\epsilon]\}\frac{\cos\theta}{z_{PQ}}\ \epsilon\ d\theta \tag{A2.7}$$

Now for Q on the circle ∂C_o we have $z_{PQ} = -\epsilon e^{i\theta}$ so the last integral can be estimated and combined with the previous relations to obtain

$$I_1' = -\frac{f_o}{2} + O[\epsilon] + \int_{A-C_o} fS''dA \qquad \text{(A2.8)}$$

If the size of the circle tends to zero, then the $O[\epsilon]$ term is negligible and the integral of equation (A2.8) tends to the limit of the integral over the punctured region.

For numerical work involving a rectangular grid it is necessary to use a rectangular neighborhood as sketched in Fig. A2.2. The same type of development leads to a formula like A2.8 except that the term $-f_o/2$ is replaced by $-f_o\, 2\theta_o/\pi$ where θ_o is the corner angle of the mesh in Fig. A2.2.

$$\tan \theta_o = \left| \frac{dy}{dx} \right| \qquad \text{(A2.9)}$$

In the case of a square element $\theta_o = \pi/4$ and the result is the same as for a circle.

III. A Finite Difference Scheme for Transverse Shear Problems

Introduction

In this chapter we consider the numerical solution of the problem of the half-space $y \geq 0$ under the parabolic transverse shear loading given by (1.27). The fully elastic solution for this problem is given by (1.28) and (1.29). Here we assume a material having a bilinear equivalent stress-total strain curve i.e., a material which strain hardens linearly.

The stress components can be expressed in terms of a potential function $\varphi(x,y)$ by (1.17). The function φ satisfies (1.18) with λ given by (1.19)-(1.21). For convenience, we normalize all stress components with respect to the initial yield stress in pure shear τ_o. That is, we take τ_o to be unity in (1.19). We shall discuss the numerical solution of the system of equations (1.18)-(1.21) here.

Nature of the Equation for φ

In the elastic region, where λ is identically zero, the differential equation (1.18) for φ reduces to Laplace's equation.

In the plastic region, λ is given by

$$\begin{aligned} \lambda &= \beta(1 - \tau^{-1}) \\ \tau &= (\varphi_x^2 + \varphi_y^2)^{\frac{1}{2}} \end{aligned} \tag{3.1}$$

Differentiating λ partially with respect to x and y, substituting in (1.18) and simplifying gives

$$[1 + \beta(1-\tau^{-1}) + \beta\varphi_x^2\tau^{-3}]\varphi_{xx} + [1 + \beta(1-\tau^{-1}) + \beta\varphi_y^2\tau^{-3}]\varphi_{yy} + 2\beta\tau^{-3}\varphi_x\varphi_y\varphi_{xy} = 0 \tag{3.2}$$

The nature of this partial differential equation of the second order is determined by the behavior of the function

$$\Delta = [\beta\tau^{-3}\varphi_x\varphi_y]^2 - [1+\beta(1-\tau^{-1}) + \beta\varphi_x^2\tau^{-3}][1+\beta(1-\tau^{-1}) + \beta\varphi_y^2\tau^{-3}]$$

Simplifying and rearranging gives

$$\Delta = -[1 + \beta(1-\tau^{-1})]^2 - [1 + \beta(1-\tau^{-1})]\beta\tau^{-1} \tag{3.3}$$

This expression is negative definite in the yielded region since $\lambda \geq 0$ throughout the plastic region. Thus, equation (1.18) is elliptic throughout (in the plastic region as well as in the elastic region).

Numerical Solution

We consider the numerical solution of the elastic-plastic transverse shear problem for the half-space $y \geq 0$ with the boundary loading given by (3.1). In view of the symmetry of the boundary loading it is sufficient to consider the quarter space $x \geq 0$, $y \geq 0$. This leads to the solution of equation (1.18) in the first quadrant with suitable boundary conditions along the x and y axes.

The boundary condition on the xz-plane, viz

$$\tau_y = \varpi_x = \begin{cases} 0 & , |x| > 1, \ y = 0 \\ \tau_m(1-x^2), & |x| < 1, \ y = 0 \end{cases}$$

leads to the conditions on the x axis:

$$\varphi = \begin{cases} 0 & , |x| > 1 \\ \frac{\tau_m}{3}(x-1)^2(x+2), & |x| < 1 \end{cases} \tag{3.4}$$

On the yz plane, because of symmetry, we have

$$\tau_x = \varphi_y = 0$$

This leads to the boundary condition

$$\varphi = \text{constant} = \frac{2}{3}\tau_m, y > 0,\ x = 0 \tag{3.5}$$

on the y axis.

We next set up a finite difference scheme for the solution of (1.18). Instead of considering the entire first quadrant, we consider the finite rectangle R:

$$R = \{(x,y):\ 0 \leq x \leq a,\ 0 \leq y \leq b\} \tag{3.6}$$

If the yielded region is very small and close to the origin, it follows from the integral equation formulation of Chapter I that at large distances from the yielded region, the solution is essentially that of the fully elastic problem. (Mendelson [7] assumes this result without proof.) Thus we are justified in imposing as boundary conditions on the edges $x = a$ and $y = b$ of the rectangle, the fully elastic solution.

We next describe the finite difference scheme used to solve equation (1.18). The rectangle $0 \leq x \leq a,\ 0 \leq y \leq b$ is divided into MN square meshes by means of the straight lines

$$\begin{aligned} x &= jh \qquad j = 1, 2, \ldots M - 1 \\ y &= ih \qquad i = 1, 2, \ldots N - 1 \end{aligned} \tag{3.7}$$

where $a = Mh$ and $b = Nh$. This gives $(M-1) \times (N-1)$ interior points and $2(M+N-1)$ boundary points.

Let the value of the function f at the point (qh, ph) be denoted by f_{pq}. Let $(f_x)_{pq}$, $(f_y)_{pq}$ denote the values of the partial derivatives of f at that point. If P_{ij} is an interior mesh point, we have, in finite difference form

$$(f_x)_{ij} = (f_{i,j+\frac{1}{2}} - f_{i,j-\frac{1}{2}})/h$$

$$(f_y)_{ij} = (f_{i+\frac{1}{2},j} - f_{i-\frac{1}{2},j})/h \tag{3.8}$$

Thus equation (1.18) written in finite difference form is

$$[(1+\lambda)\frac{\partial \varphi}{\partial x}]_{i,j+\frac{1}{2}} - [(1+\lambda)\frac{\partial \varphi}{\partial x}]_{i,j-\frac{1}{2}} + [(1+\lambda)\frac{\partial \varphi}{\partial y}]_{i+\frac{1}{2},j} - [(1+\lambda)\frac{\partial \varphi}{\partial y}]_{i-\frac{1}{2},j} = 0 \tag{3.9}$$

In terms of the values of φ and λ at the mesh points we can write this equation in the form

$$\varphi_{i,j+1}[1+\tfrac{1}{2}(\lambda_{i,j}+\lambda_{i,j+1})] + \varphi_{i,j-1}[1+\tfrac{1}{2}(\lambda_{i,j}+\lambda_{i,j-1})] + \varphi_{i+1,j}[1+\tfrac{1}{2}(\lambda_{i,j}+\lambda_{i+1,j})]$$

$$+ \varphi_{i-1,j}[1+\tfrac{1}{2}(\lambda_{i,j}+\lambda_{i-1,j})] - \varphi_{i,j}[4+\tfrac{1}{2}(4\lambda_{i,j}+\lambda_{i,j+1}+\lambda_{i,j-1}+\lambda_{i+1,j}+\lambda_{i-1,j})] = 0 \tag{3.10}$$

The procedure used for solving these equations is described next.

Let $\varphi_{ij}^{(n)}$ denote the values of φ_{ij} after the n^{th} iteration. The corresponding values of λ_{ij} are calculated from the equations

$$\lambda_{ij}^{(n)} = \beta[1 - 1/(\tau)_{ij}^{(n)}] \tag{3.11}$$

$$(\tau)_{ij}^{(n)} = \left[(\varphi_{i,j+1}^{(n)} - \varphi_{i,j-1}^{(n)})^2 + (\varphi_{i+1,j}^{(n)} - \varphi_{i-1,j}^{(n)})^2\right]^{1/2}/h \tag{3.11}$$

During the (n+1)st iteration $\varphi_{ij}^{(n+1)}$ values are obtained by a "row by row" procedure. That is, we solve for $\varphi_{1j}^{(n+1)}$ (j = 1, 2, ... M-1) first, then for $\varphi_{2j}^{(n+1)}$ (j = 1, 2, ..., M-1), and so on.

The $\varphi_{ij}^{(n+1)}$ values for row i are obtained as follows. These are assumed to satisfy the linear equation

$$a_j \varphi_{i,j-1}^{(n+1)} + b_j \varphi_{i,j}^{(n+1)} + c_j \varphi_{i,j+1}^{(n+1)} = d_j \tag{3.12}$$

where

$$\begin{aligned}
a_j &= 1 + \frac{1}{2}(\lambda_{i,j}^{(n)} + \lambda_{i,j-1}^{(n)}) \\
c_j &= 1 + \frac{1}{2}(\lambda_{i,j}^{(n)} + \lambda_{i,j+1}^{(n)}) \\
b_j &= -4 - \frac{1}{2}(4\lambda_{i,j}^{(n)} + \lambda_{i,j+1}^{(n)} + \lambda_{i,j-1}^{(n)} + \lambda_{i-1,j}^{(n)} + \lambda_{i+1,j}^{(n)}) \\
d_j &= -\varphi_{i+1,j}^{(n)}\left[1 + \frac{1}{2}(\lambda_{i,j}^{(n)} + \lambda_{i+1,j}^{(n)})\right] - \varphi_{i-1,j}^{(n+1)}\left[1 + \frac{1}{2}(\lambda_{i,j}^{(n)} + \lambda_{i-1,j}^{(n)})\right]
\end{aligned} \tag{3.13}$$

For each "interior point" (j = 1, 2, ... M-1) we have an equation of the form (3.12). The two equations corresponding to j = 1 and j = M-1 involve the known values of φ on the boundary. Hence these two equations may be written

$$\begin{aligned}
b_1 \varphi_{i,1}^{(n+1)} + c_1 \varphi_{i,2}^{(n+1)} &= d_1 - a_1 \varphi_{i,0} = d_1' \\
a_{M-1} \varphi_{i,M-2}^{(n+1)} + b_{M-1} \varphi_{i,M-1}^{(n+1)} &= d_{M-1} - c_{M-1} \varphi_{i,M} = d_{M-1}'
\end{aligned} \tag{3.14}$$

where

$$\varphi_{i,0} = (\varphi_e)_{i,0}$$

$$\varphi_{i,M} = (\varphi_e)_{i,M} \tag{3.15}$$

The set of M-1 equations for the M-1 unknowns $\varphi_{i,j}^{(n+1)}$ (j = 1, 2, ... M-1) can be written in the form

$$A\ \Phi_i^{(n+1)} = d \tag{3.16}$$

where $\Phi_i^{(n+1)}$ and d are the column vectors

$$\Phi_i^{(n+1)} = \begin{bmatrix} \varphi_{i,1}^{(n+1)} \\ \varphi_{i,2}^{(n+1)} \\ \cdot \\ \cdot \\ \cdot \\ \cdot \\ \varphi_{i,M-1}^{(n+1)} \end{bmatrix} \qquad d = \begin{bmatrix} d_1' \\ d_2 \\ d_3 \\ \cdot \\ \cdot \\ \cdot \\ d_{M-2} \\ d_{M-1}' \end{bmatrix} \tag{3.17}$$

and A is the tri-diagonal matrix

$$A = \begin{bmatrix} b_1 & c_1 & & & & \\ a_2 & b_2 & c_2 & & 0 & \\ & a_3 & b_3 & c_3 & & \\ & & \cdot & & & \\ & & & \cdot & & \\ & & & & \cdot & \\ & 0 & & & a_{M-2}\ b_{M-2}\ c_{M-2} & \\ & & & & a_{M-1}\ b_{M-1} & \end{bmatrix} \tag{3.18}$$

The tridiagonal form of A enables us to solve equation (3.16) readily (Isacson & Keller [9]). A can be factorized in the bidiagonal form

$$A = LU = \begin{bmatrix} \alpha_1 & 0 & 0 & & \\ a_2 & \alpha_2 & 0 & 0 & \\ 0 & a_3 & \alpha_3 & & \\ & 0 & & & \\ & & & a_{M-1} & \alpha_{M-1} \end{bmatrix} \begin{bmatrix} 1 & \gamma_1 & & 0 & \\ & 1 & \gamma_2 & & \\ & & & & \\ & 0 & & \gamma_{M-2} & \\ & & & 1 & \end{bmatrix} \tag{3.19}$$

where

$$\begin{aligned} \alpha_1 &= b_1 \\ \gamma_1 &= c_1/\alpha_1 \\ \alpha_i &= b_i - a_i \gamma_{i-1} \quad , i = 2, 3, 4, \ldots M-1 \\ \gamma_i &= c_i/\alpha_i \qquad\quad , i = 2, 3, \ldots M-2 \end{aligned} \tag{3.20}$$

provided all α_i's are nonzero.

Then eq (3.16) takes the form

$$L\, U\, \Phi_i^{(n+1)} = d \tag{3.21}$$

The solution of the "intermediate equation"

$$L\, g = d \tag{3.22}$$

where

$$U\, \Phi_i^{(n+1)} = g$$

can be written

$$\begin{aligned} g_1 &= d_1'/\alpha_1 \\ g_i &= (d_i - a_i g_{i-1})/\alpha_i \quad , \; i = 2, 3, \ldots M-2 \\ g_{M-1} &= (d_{M-1}' - a_{M-1}\, g_{M-2})/\alpha_{M-1} \end{aligned} \tag{3.23}$$

Finally, the solution of (3.16) is given by

$$\varphi_{i,M-1}^{(n+1)} = g_{M-1}$$

$$\varphi_{i,j}^{(n+1)} = g_j - \gamma_j \varphi_{i,j+1}^{(n+1)}, \quad j = M-2, M-3, \ldots 1. \tag{3.24}$$

The procedure described above gives the $\varphi_{ij}^{(n+1)}$ values for points on the ith row. This procedure is carried out for rows $i = 1,2,3,\ldots$ in succession. Initially, for $n = 0$, the elastic solution is assumed:

$$\begin{aligned} \varphi_{ij}^{(0)} &= (\varphi_e)_{ij} \\ \lambda_{ij}^{(0)} &= 0 \end{aligned} \tag{3.25}$$

where $(\varphi_e)_{ij}$ denotes the value of the stress function for the fully elastic problem evaluated at the point P_{ij}.

At each iteration the following quantity

$$\Delta^{(n+1)} = \max_{i,j} |\varphi_{i,j}^{(n+1)} - \varphi_{i,j}^{(n)}| \tag{3.26}$$

was calculated, and the convergence of the sequence $\{\Delta^{(n)}\}$ gives an estimate of the convergence of the iterative scheme discussed above.

IV An Attempted Simple Description of the Plastic Deformation Near a Crack Tip

The goal of this effort was to study the possibility of establishing a simple fracture criterion based upon a modified Dugdale model which includes material strain hardening parameters. In order to reduce tedious mathematical details which only obscure the physics, the first studies were made for the case of transverse shear or mode III deformations instead of direct tension or mode I loading. An example is discussed in more detail in this chapter.

In the Dugdale type model the effect of the plastically yielded zone ahead of the crack tip is approximated by a mathematical problem with a crack which extends through the plastic region. The configuration is shown in Fig. 4.1.

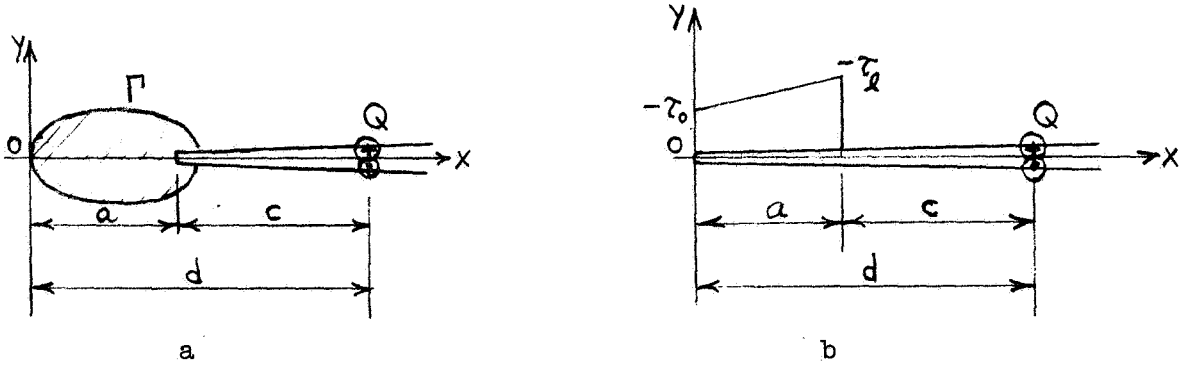

Fig. 4.1 The plastic region and the Dugdale model.

In the Dugdale model the entire cut plane is assumed to behave elastically, and the effect of the plastic zone is approximated by τ_o, the initial yield stress in shear, acting on the segment $0 \leq x \leq a$. A slight modification of the Dugdale model is suggested in Fig. 4.1.b where the stress increases linear-

ly from $-\tau_o$ to $-\tau_\ell$ the ultimate shear stress at the end of the real crack at $(a,0)$.

For simplicity we consider an example of loading by concentrated opposed shear forces Q acting perpendicular to the x-y plane on the edges of the cut at $(d,0)$. For initial yielding the high stress regions near the loads Q are coupled only very weakly with the region of the crack tip and hence they can be ignored.

This problem for the cut elastic plane can be solved by complex variable methods, see Mushkelishvilli [11], or by a combination of integral transforms and complex variables, see Baker [12]. It can be verified that the following complex stress functions give the solution of the elastic problem.

$$F(z) = \tau_y + i\tau_x = \frac{i}{\pi}\left\{\frac{Q}{z-d}\sqrt{\frac{d}{z}} + \frac{Q}{\sqrt{zd}} + \right.$$

$$\left. + \tau_o\left[2\delta\sqrt{\frac{z}{a}} - \left(1 + \frac{z}{a}\delta\right)\ln\frac{\sqrt{z}+\sqrt{a}}{\sqrt{z}-\sqrt{a}}\right]\right\}$$

$$F_o(z) = -\varphi + iGw = \frac{i}{\pi}\left\{Q\ln\frac{\sqrt{z}-\sqrt{d}}{\sqrt{z}+\sqrt{d}} + \tau_o(2+\frac{\delta}{3})\sqrt{az} + a\tau_\theta\delta\left(\frac{z}{a}\right)^{3/2}\right. \tag{4.1}$$

$$\left. -a\tau_\theta\left[1 + \delta\,\frac{z+a}{2a}\right]\frac{z-a}{a}\ln\frac{\sqrt{z}+\sqrt{a}}{\sqrt{z}-\sqrt{a}}\right\}$$

where

$$\delta = \frac{\tau_\ell - \tau_o}{\tau_o}$$

Dugdale required that stresses be finite at the origin to determine the length a of the plastic zone. That condition has already been incorporated in equation (4.1) and is

$$\frac{Q}{\sqrt{ad}\,\tau_o} = 2 + \frac{2}{3}\delta \tag{4.2}$$

This finite stress criterion determines the plastic zone size, but it does not give a failure criterion. In fact, if Q increases for a fixed d then a also increases without limit.

We note two important features of the elastic solution. There is a logarithmic singularity in stresses at the end of the loaded region a. This phenomenon occurs in all elasticity problems at points of the boundary where the applied stresses are discontinuous. That singularity could be eliminated by modifying the boundary load, say by adding a linear variation of stress from τ_o down to zero over a small interval.

Another important point is that relative slipping occurs across the loaded interval $y = 0,\ 0 \leq x \leq a$. The loads Q shear those edges apart. The local shear stresses acting on the segment tend to pull the edges back together, but the local deformation is not enough to heal the cut.

However, the yielded material deforms more readily so the plastic plug of the actual body does have continuous displacements across the segment $0 \leq x \leq a$. The simple model which we proposed to investigate consists of a crude approximation of the deformations in the plastic plug. Those deformations are to be adjusted to provide continuity of displacement and stresses at Γ, the interface between the elastic and plastic regions.

A simple expansion was proposed for the stress function in the plastic region. The compatability equation (1.18) is

$$(1+\lambda)\,\nabla^2\varphi + \lambda_x\,\varphi_x + \lambda_y\,\varphi_y = 0 \tag{4.3}$$

This equation applies in the region bounded by Γ and the x-axis, see Fig. 4.2.

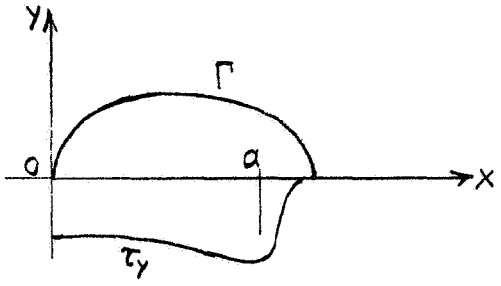

Fig. 4.2 The Plastic Region and Smooth Boundary Values.

As was noted in Chapter III the partial differential equation (4.3) is elliptic. The Cauchy-Kowaleskii theorem, see Sneddon [8] or Courant and Hilbert [13], states that for such an equation with given analytic boundary data on an analytic curve, that the solution can be expanded in a convergent Taylor series in a region adjacent to the given curve.

Estimates of the rate of convergence are generally very difficult, but the theorem does support the use of an expansion of the following type,

$$\varphi(x,y) = f_o(x) + y^2 f_2(x) + y^4 f_4(x) + \ldots \tag{4.4}$$

The stress potential is even in y because of the symmetry of the problem.

The corresponding stresses are

$$\begin{aligned} \tau_x &= \varphi_{,y} = 2y\, f_2(x) + 4y^3 f_4(x) + \ldots \\ -\tau_y &= \varphi_{,x} = f_o'(x) + y^2 f_4'(x) + \ldots \end{aligned} \tag{4.5}$$

The stress distribution used in the elastic solution (4.1) is certainly not analytic at $x = a$ where there is a discontinuity. However, the stresses are bounded in the plastic zone for any real material and must be distributed approximately as shown in Fig. 4.2.

For any smooth distribution of this type there is an analytic function which closely approximates it. Then we can appeal to the continuous dependence of the solution of an elliptic equation upon boundary data to argue that the deformation at the interface Γ is only slightly changed by this smoothing process. However, the two distributions must be statically equivalent.

With the preceding arguments we can use the simple expansion (4.4) to obtain the solution at least in a narrow region near the x-axis. Substitution into the compatability equation (4.3) and comparison of powers of y gives relations between successive functions $f_o(x)$, $f_2(x)$, ... The analytic function $f_o(x)$ whose derivative is the negative of the given stress $\tau_y(x,0)$ on the initial curve can be specified arbitrarily. Then the next function $f_2(x)$ is given by

$$f_2 = -\frac{f_o''}{2}\frac{(1+\beta)f_o'}{\beta+(1+\beta)f_o}, \tag{4.6}$$

and successive functions are obtained from similar but more complicated relations.

It is conceivable that the boundary stress, or function f_o, could be varied in a systematic manner say by altering the coefficients of a polynomial of given degree for both the plastic solution and the elastic solution until the stress components and displacement agree at interface Γ.

As a very crude approximation of such a process the matching was only enforced at the point (a,y_Γ) where the line $x = a$ intersects the interface Γ. The stress τ_y was truncated after the second term so that it varies parabolically on $x = a$:

$$\tau_y(a,y) = \tau_\ell - \frac{y^2}{y_\Gamma^2}[\tau_\ell - \tau_y(a,y_\Gamma)] \equiv a_o - a_2 \frac{y^2}{y_\Gamma^2} \tag{4.7}$$

The function $\lambda(a,y)$ was also truncated in parabolic form. It varies from its maximum value on the x-axis down to zero on Γ.

$$\lambda(a,y) = \beta(1 - \frac{1}{\tau_\ell})(1 - \frac{y^2}{y_\Gamma^2}) \equiv \lambda_a(1 - \frac{y^2}{y_\Gamma^2}) \tag{4.8}$$

The displacement at the interface is found by integrating equation (1.14) for the total strain

$$G\, w(a,y_\Gamma) = \int_0^{y_\Gamma} (1+\lambda)\tau_y dy$$

$$= y_\Gamma\{(1+\lambda_a)a_o - [\lambda_a a_o + a_2(1+\lambda_a)]\frac{1}{3} + \lambda_a a_2 \frac{1}{5}\} \tag{4.9}$$

Compatability of the simple elastic solution (4.1) and the crude plastic approximations (4.7-4.9) was enforced in an inverse computational method. The distance c to the applied loads along the free surface of the crack was chosen as a fixed reference length, and the plastic zone length a and the stress difference $\tau_\ell - \tau_o$ were varied. The corresponding value of Q was determined from the finite stress condition (4.2), and this specified the elastic solution.

From the elastic solution the point (a,y_Γ) was determined, and the corresponding stress $\tau_y(a,y_\Gamma)$ and displacement $w(a,y_\Gamma)$ were computed. These values were substituted into the system of equations (4.7) to (4.9) to find β, the remaining material parameter, which would give compatability at the point.

The results, shown in Fig. 4.3, are disappointing. The dependence of the load Q upon the plastic zone size a is only moderately affected by changes in δ, a measure of the ultimate strength, which is reasonable. However, β, a measure of stiffness in the plastic range, depends primarily upon δ and not upon the yield zone size a. This indicates that the simple truncated representation of stresses is not adequate.

It had been expected that such gross deformation features could be used to modify the Dugdale model to introduce a failure criterion. It still is reasonable that a better representation of the deformations in the plastic plug could be obtained by using more terms in the expansion (4.4) and by adding self equilibrating polynomial distributions of shear stress to the loaded interval $0 \leq x \leq a$ in the elastic solution. These parameters would be determined by enforcing compatability at more points on the interface.

Preliminary attempts were made to develop this type of point matching technique for the types of problems considered in Chapters II and III. However, a simple computational scheme was not found, and the methods considered were very tedious to code. A feasible program was not developed.

Nevertheless, the feasibility study of this chapter did bring out several features which show that such solutions, even if available, would still not lead to a reasonable failure criterion. In particular, the boundedness

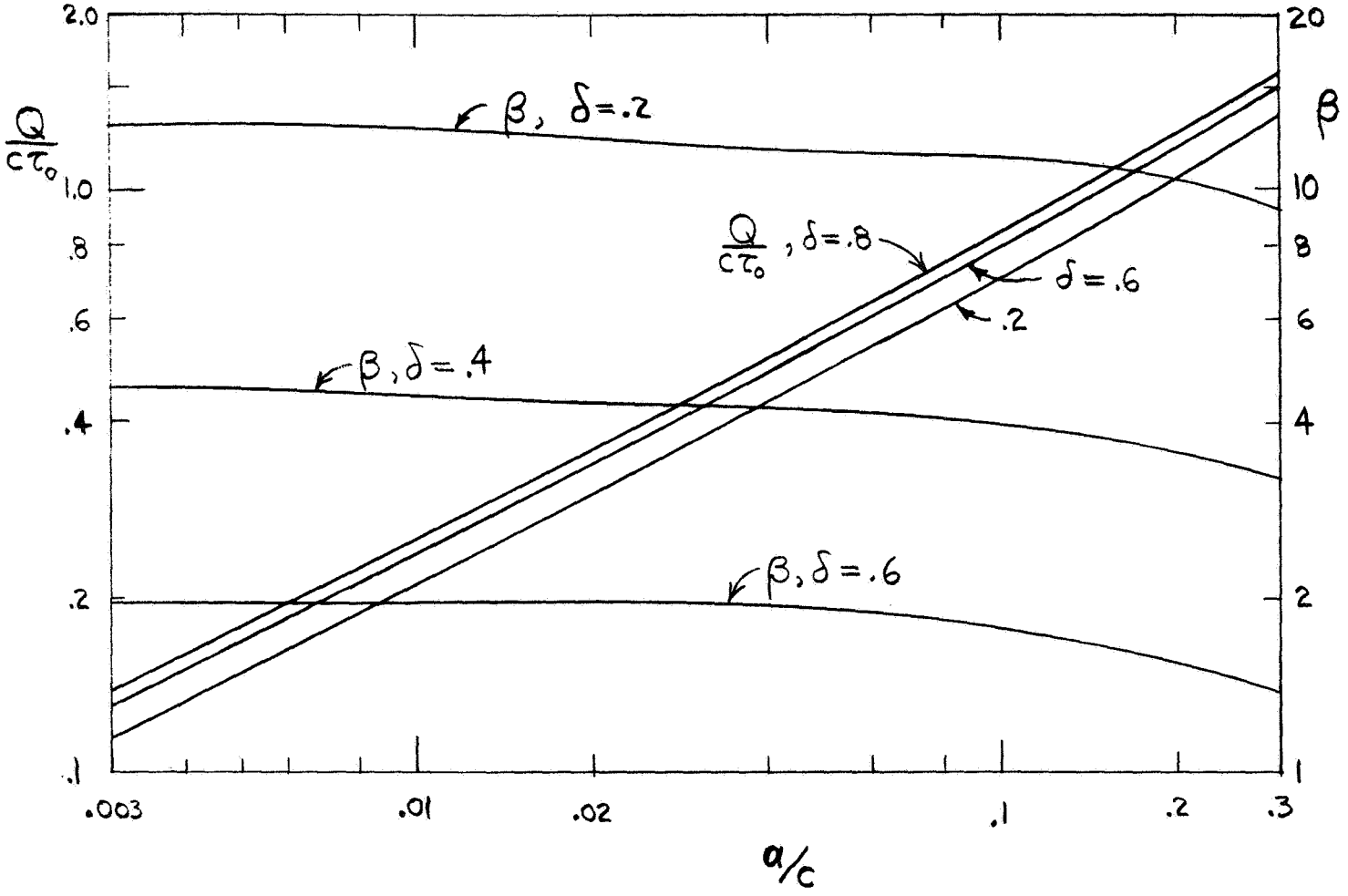

Fig. 4.3. Load Level and Strain Hardening Parameter as Functions of Yield Zone Length.

and analyticity of the stresses at the end of the real crack play important roles in physically realistic failure criteria.

Recent works by Rice[2,5] and Hutchinson[3,4] show stress singularities at the ends of crack tips in strain hardening materials. The presence of infinite stresses in continuum mechanics violates our most intuitive notions of strength.

In the next chapter these questions are discussed in more detail. It appears that not only the strain hardening characteristics of the continuum representation of a material are necessary, but a better representation of the microstructure at a crack tip is required to establish a failure criterion.

V Failure Criteria

The original purpose of this investigation was to determine the influence of the strain hardening parameters of a material upon its fracture resistance. However, some of the questions of boundedness of stresses which arose in the last chapter suggest that a better description of the microstructure at a crack tip will be necessary in order to define a significant fracture criterion. At this point we will review some useful fracture criteria for brittle materials to provide a background for discussion of ductile materials.

In his original work Griffith [14] utilized an energy criterion to determine an unstable or critical crack size in an infinite stretched elastic plate. The conclusions agreed well with experimental results in spite of the fact that the stress distribution included a singularity at the crack tip. In fact, in later years the strength of the singularity or the stress concentration factor of a linear elastic analysis became accepted as a useful measure of the resistance of a cracked structural element made of a brittle material.

The paradox of a useful failure criterion involving infinite stresses has been clarified by Barenblatt [15], [16]. Barenblatt's analysis accounted for the intermolecular cohesive forces which act near the end of a crack in a brittle elastic material. As indicated in Fig. 5.1, the end of the crack closes smoothly so the opposite faces of the crack are very close in the end zone. Therefore, intermolecular attractions are effective near the end of the crack. However, where the opening of the crack is greater the mean attraction or stress falls off as indicated in Fig. 5.1.b.

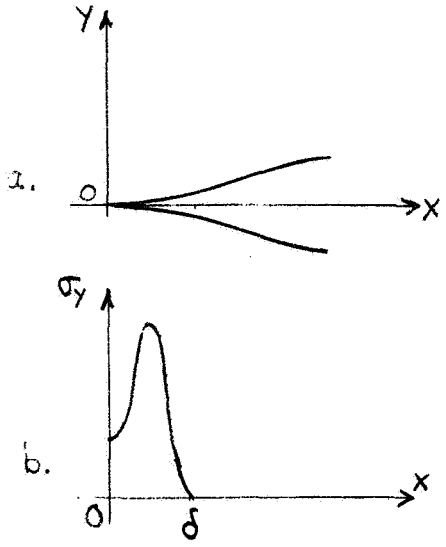

Fig. 5.1 The Barenblatt Model for a brittle elastic material

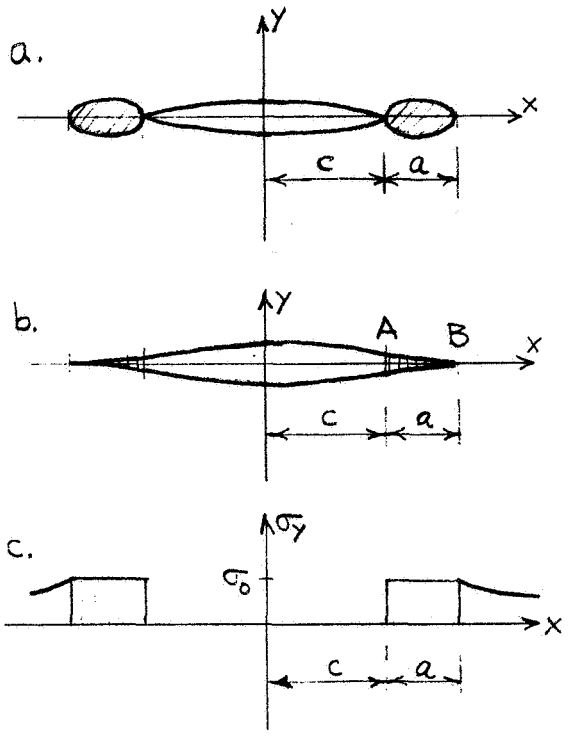

Fig. 5.2 The Dugdale Model

The effect of these additional intermolecular forces is to pinch the ends of the crack together. In terms of the linear theory of elasticity the applied or external loads produce a tensile stress singularity at the crack tip or a positive stress intensity factor. The cohesive or internal stresses produce a compressive singularity or a negative stress intensity factor. Superposition of the two effects is valid in the linear theory, so the singularities can cancel each other and leave a finite stress system.

Apparently for a given material at a given temperature there is a maximum pinch which the cohesive stresses can exert. This pinch is a material parameter which gives the maximum attainable value of the stress intensity factor. If the applied loads produce a greater intensity then the crack must grow.

This model provides a good description of a tensile test of a brittle material. The overall or gross behavior is that the applied loads vary linearly with observable deformations right up to the point of rapid fracture.

A ductile material is represented better by the model proposed by Dugdale [10] and utilized in the last chapter. Dugdale noted that the plastic zones near crack tips in very ductile sheets which were loaded in tension appear to be slender regions extending ahead of the crack as indicated in Fig. 5.2.a.

The stress measured in a bar tensile test of a ductile material is never much greater than the initial yield stress σ_o. Noting this fact and the shape of the yield zones, Dugdale introduced a mathematical model, shown in Fig. 5.2.b, with a crack extending through the actual plastic zones of Fig. 5.2.a. The normal stress σ_y is set equal to the initial yield stress σ_o on the "plastic interval" a of the longer mathematical crack.

In the Dugdale model the external loads, for example uniform tension $\sigma_y \equiv T$ at infinity, also produce tensile stress singularities at the ends of the mathematical crack of length $2c + 2a$. The stress σ_o acting on the plastic interval a produces a compressive singularity. Cancellation of the singularities is used as a condition to determine the length a.

The size of the plastic zone determined by these methods does agree well with experimental results obtained by Dugdale and by several subsequent investigators. However, the analysis does not lead to a failure criterion; if the applied load T increases toward σ_o then the size of the yield zone grows indefinitely.

Other authors have attempted to incorporate the strain hardening results of tensile tests into a modified Dugdale model. For example Goodier and Field [17] defined a measure of strain as the ratio of the opening of the Dugdale crack at point A of Fig. 5.2.b divided by a "gage length" 2d. It would be desirable to compare this measure with the strain at failure in tensile tests.

However, the gage length is not deduced from other dimensions of the body or from material properties, so it must be determined from experimental results. There is no evidence to suggest that the gage length is a universal material constant.

A more detailed attack has been made by Rice [2,18] and Hutchinson [3, 4] who have studied the stress singularities at the end of a crack in a plastic region. Both of these authors have made extensive use of a path independent integral which was developed by Eshelby [19] and was rediscovered by Rice and by Cherepanov [20].

The invariant integral is

$$J = \int_{\Gamma} \left(w \, dy - \bar{T} \cdot \frac{\partial \bar{u}}{\partial x} \, ds \right) \tag{5.1}$$

where the strain energy density at a point is

$$w = w(x,y) = w(\epsilon) = \int_{0}^{\epsilon_{ij}} \sigma_{ij} \, d\epsilon_{ij} \tag{5.2}$$

$\bar{T}$ is the traction vector acting on the material contained by the contour Γ, and $\bar{u}$ is the displacement vector. The contour Γ encircles the end of a flat sided notch as shown in Fig. 5.3.

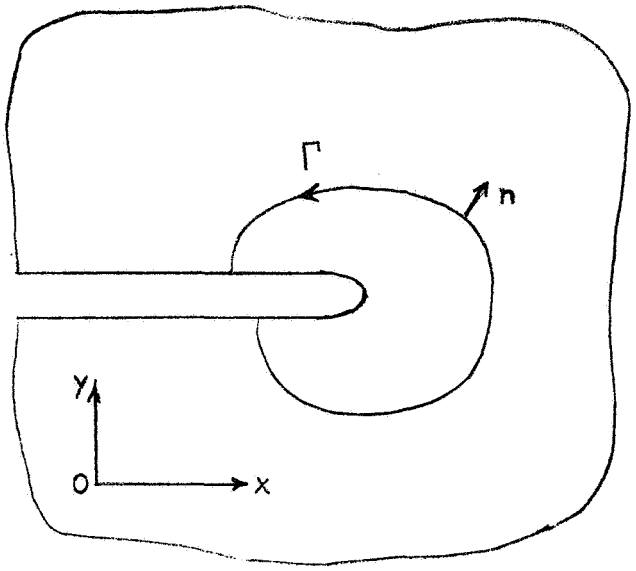

Fig. 5.3 A Flat Sided Notch

The derivation of the path independent integral requires that Γ passes from a point on the lower flat surface of the notch to a point on the upper flat surface. In addition Γ must lie in a portion of the elastic medium free of singularities. On flat stress-free segments of the notch faces the integrand of (5.1) vanishes. Hence, the end points of Γ can be moved along such segments with no change in J. Rice has shown that it is often possible to evaluate J by choosing a path Γ where the integrand is known. Sometimes this path is the boundary of the cracked body.

If the notch is a flat stress-free crack, then Γ can be shrunk down to a small circle around the crack tip and J has the form

$$J = r \int_{-\pi}^{\pi} \{w[\varepsilon(r,\theta)] \cos\theta - \overline{T}(r,\theta) \cdot \frac{\partial \overline{u}}{\partial x}(r,\theta)\} d\theta \qquad (5.3)$$

Since r can tend to zero, the integrand must have a singularity of the order $1/r$. In a linear elastic material the stresses are proportional to strains so both would have the characteristic $r^{-1/2}$ singularity.

Introduction of cohesive stresses in a small end zone of length δ requires modification of the limiting procedure. Now the traction $\bar{T}$ is non-zero so the integral over the flat end region must be retained. On the other hand, if stresses are finite at the tip then the integral of (5.3) is bounded and the product with r vanishes in the limit. Then the value of J is

$$J = 2 \int_0^{\delta} \sigma_y(r') \frac{\partial v}{\partial r'} \, dr' \tag{5.4}$$

It can be shown in linear elasticity theory that a finite stress system at the origin leads to a crack opening with the asymptotic form

$$v \sim a r^{1/2} \tag{5.5}$$

so

$$J = a \int_0^{\delta} \frac{\sigma_y(r')}{\sqrt{r'}} \, dr' \tag{5.6}$$

The last integral is proportional to Barenblatt's modulus of cohesion, a material property.

Similar techniques can be used to study the stress and strain state at the end of a crack in a ductile medium, but certain modifications are necessary.

Rice has argued appropriately that deformation theory can be used under conditions of proportional loading which are satisfied for initial plastic yielding. Under these conditions the deformation theory is really equivalent to non-linear elasticity, and the derivation of the J integral is still valid.

Infinite stresses, of course, are still unreasonable even for a plastic or non-linear elastic material. The singularity can be eliminated, as in the elastic case, if we introduce cohesive stresses near the crack tip in order to provide a reasonable continuum representation of the microstructure where fracture occurs.

It can be expected that the continuum approximation of the crystal structure must be invalid at the crack tip where grains and impurities must begin to pull apart. In fact, experimental work by Rogers [21] and Puttick [22] show a fibrous microstructure where voids appear near the end of a crack. The appearance is indicated in Fig. 5.4.

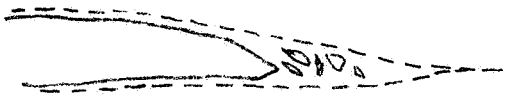

Fig. 5.4 The Fibrous Zone at a Crack Tip.

It seems reasonable to use continuum mechanics for the region outside the dashed lines, but not in the shredded zone just ahead of the crack. A useful representation of that zone probably could be made in terms of cohesive stresses acting on the end of the sharp crack indicated by dashed lines. The effective pinch exerted by those fibers could probably be described conveniently by an integral like that of equation (5.4).

A representation of this type would parallel the description used for brittle elastic materials. However, there is one very important difference for the plastic or nonlinear elastic material. Because of the nonlinearity

of the system it is not permissible to use superposition. Therefore, stress or strain concentrations cannot be added, and the usefulness of a stress intensity factor as failure criterion is highly doubtful. It appears that more convenient but detailed methods of analysis must be developed for the nonlinear problems.

When such a localized pinch is used we expect that the cohesive stresses near the crack tip must be very large as they are in the Barenblatt brittle model. This seems to contradict the well known behavior of ductile materials in tensile tests where the mean stress is never much larger than the initial yield stress, σ_o. However, those test results only give the mean stress but no details of the stresses near microcracks in the specimen. Similar remarks apply to tensile tests of brittle materials; fracture occurs at a mean stress far below the level of cohesive stresses.

VI Conclusions

Problems of the first kind for the deformation theory of plasticity have been studied. Tractable numerical methods based upon finite difference equations and upon a nonlinear integral equation formulation were developed. The integral equation approach apparently has not been used before in the theory of plasticity. It is a potentially useful tool and should be developed further.

Crude approximate attempts to obtain the stress distribution in the plastic region near the crack tip revealed the importance of the description of the microstructure in the region where tearing occurs. We conclude that this description is as essential as the strain-hardening continuum representation of the material for the establishment of a useful failure criterion.

Although the stress concentration method is useful for linearly elastic brittle materials, it does not seem feasible for ductile materials. The plastically deformed material behaves in a highly nonlinear manner, so that superposition is not valid.

It appears that more convenient approximate methods of solution must be developed for problems of a nonlinear continuum. Perhaps such methods could be combined with approximate descriptions of the microstructure to derive a fracture criterion in a form useful for engineering design.

References

1. Rice, J. R., "Contained Plastic Deformation Near Cracks and Notches Under Longitudinal Shear," I. J. Frac. Mech., 1966, 2, pp 426-447.

2. Rice, J. R., "Stresses Due to a Sharp Notch in a Work-Hardening Elastic-Plastic Material Loaded by Longitudinal Shear," JAM, 1967, 34, pp 287-298.

3. Hutchinson, J. W., "Singular Behavior at the End of a Tensile Crack in a Hardening Material," J. Mech. Phys. Solids, 1968, 16, pp 13-31.

4. Hutchinson, J. W., "Plastic Stress and Strain Fields at a Crack Tip," J. Mech. Phys. Solids, 1968, 16, pp 337-347.

5. Rice, J. R. and Rosengren, G. F., "Plane Strain Deformation Near a Crack Tip in a Power-Law Hardening Material," J. Mech. Phys. Solids, 1968, pp 1-12.

6. Budiansky, B., "A Reassessment of Deformation Theories of Plasticity," JAM, 1959, 81E, pp 258-264.

7. Mendelson, A., Plasticity: Theory and Application, MacMillan, New York, 1968.

8. Sneddon, I. N., Elements of Partial Differential Equations, McGraw Hill, New York, 1957.

9. Isaacson, E. and Keller, H. B., Analysis of Numerical Methods, Wiley, New York, 1966.

10. Dugdale, D. S., "Yielding of Steel Sheets Containing Slits," J. Mech. Phys. Solids, 1960, 8, pp 100-104.

11. Muskhelishvilli, N. I., Some Basic Problems of the Mathematical Theory of Elasticity, P. Nordhoff, Groningen, 1953.

12. Baker, B. R., "Tearing of Viscous Fibers", Int. J. Fracture Mech., 1968, pp. 371-382, also in Russian in Mekhanika Tverdovo Tela, Academy of Sciences, U.S.S.R., 1969, pp. 113-121.

13. Courant, R. and Hilbert D., Methods of Mathematical Physics, Vol. 2 Interscience, New York, 1962.

14. Griffith, A. A., "The Phenomena of Rupture and Flow in Solids," Phil. Trans. Roy. Soc. (London), 1921, A221, p. 163-198.

15. Barenblatt, G. I., "On the Equilibrium Cracks due to Brittle Fracture," Doklady AN SSSR, 1959, 127, pp 47-50 (in Russian).

16. Barenblatt, G. I., "Mathematical Theory of Equilibrium Cracks in Brittle Fracture," Advances in Applied Mechanics, Vol. 7, Academic Press, 1962.

17. Goodier, J. N. and Field, F. A., "Plastic Energy Dissipation in Crack Propagation," Fracture of Solids, Wiley, New York, 1963.

18. Rice, J. R. "A Path Independent Integral and the Approximate Analysis of Strain Concentrations by Notches and Cracks," JAM, 1968, 35, pp 379-386.

19. Eshelby, J. D., "The Continuum Theory of Lattice Defects," Solid State Physics, Vol. 3, Academic Press, 1956.

20. Cherepanov, G. P., "Crack Propagation in Continuous Media," PMM, 1967, 31, pp 503-512.

21. Rogers, H. C., "The Tensile Fracture of Ductile Metals," Trans. Metall. Soc. AIME, 1960, 216, pp 498-506.

22. Puttick, K. E., "Ductile Fracture in Metals," Phil. Mag. 8th Ser., 1959, 4, pp 964-969.